

## Aloe vera Rind Cellulose Nanofibers-Reinforced Films

Shuna Cheng,<sup>1</sup> Suhara Panthapulakkal,<sup>1</sup> Mohini Sain,<sup>1</sup> Abdulah Asiri<sup>2</sup>

<sup>1</sup>Centre for Biocomposites and Biomaterials Processing, Faculty of Forestry, University of Toronto, Toronto, Ontario M5S 3B3, Canada

<sup>2</sup>Centre of Advanced Chemistry, King Abdulaziz University, Jeddah, 21589, Saudi Arabia

Correspondence to: S. Cheng (E-mail: shuna.cheng@utoronto.ca)

**ABSTRACT:** *Aloe vera* (AV) gel has been widely used in various medical, cosmetic, and nutraceutical applications. However, AV rind, the tougher outer layer of AV leaves where the cell wall components exist, is currently treated as a fertilizer or waste. This study aimed to investigate the potential of the AV rind as a resource for the production of cellulose nanofibers. Since a detailed analysis of the AV rind has been lacking, chemical composition of rind was analyzed before processing it into nanofibers. The results showed that AV rind has a high proportion of  $\alpha$ -cellulose ( $57.72\% \pm 2.18\%$ ). AV rind nanofibers (AVRNF) were prepared using chemi-mechanical process. The morphological analyses showed that most of the isolated fibers were individual fibers under 20 nm. Crystallinity and degree of polymerization of the obtained AVRNF, and mechanical properties of the nanofibrous film were evaluated and compared with the wood nanofibers. Tensile strength of AVRNF film (102 MPa) was comparatively lower than the wood fibers (132 MPa), which was consistent with the lower crystallinity of AVRNF [crystallinity index (CI) = 0.66] as well as the lower degree of polymerization (DP = 396), compared with wood fibers (CI = 0.90, DP = 1297). © 2014 Wiley Periodicals, Inc. *J. Appl. Polym. Sci.* **2014**, *131*, 40592.

**KEYWORDS:** characterization; fibers; films; properties; X-ray

Received 30 August 2013; accepted 11 February 2014

**DOI:** 10.1002/app.40592

### INTRODUCTION

*Aloe vera* (AV), (*Aloe barbadensis* Miller), a desert plant, is similar to a Cactus but belongs to the Lily (Liliaceae) family. The plant was used as a drug, which can be dated back to 6000 years BC.<sup>1</sup> It is widely cultivated throughout the world as a crop for its jelly like parenchyma known as “Aloe vera gel.” The leaf mainly consists of rind, latex, and gel as shown in Figure 1. The AV gel has been widely used today in cosmetic products and in wound healing due to its anti-inflammatory properties, healing effects, mucus stimulatory effects, and regulation of gastric secretions.<sup>2–5</sup> The latex portion obtained from the pericyclic cells under the AV rind (outer skin) is commonly used in pharmaceutical industry.<sup>3</sup> AV mainly grows in the dry regions of South Texas, Florida, and South California in the United States, Mexico, India, South and Central America, Africa, Australia, Caribbean, and Iran.<sup>1</sup> If AV rind can be used as a resource for high-performing nanocellulose fibers, it would be an alternative to agro-resources, where lots of irrigation is needed. Furthermore, the use of AV rind can add more value to this plant and can promote the local economy. However, there is little information about chemical composition and utilization of AV rind that is currently being treated as a fertilizer or waste.

AV rind, consisting of 15 cell layers in thickness, has the function of protecting the gel as well as synthesizing carbohydrates, fat, and protein.<sup>6</sup> Many carbohydrates from AV such as glucose, fructose, and polysaccharides including glucomannans and polymannose have been isolated. However, separation of cellulose, part of the carbohydrate made, have not been reported yet. In this study, we tried to isolate the cellulose from the AV rind for nanofibers preparation. Several methods have been reported for the isolation of cellulose microfibrils from plant cell wall, including enzymatic, chemical, mechanical, and chemo-mechanical processes. The chemical treatment was intended to remove most of hemicellulose, lignin, pectin, and protein.

In this study, a chemo-mechanical approach was employed for the production of cellulose nanofibers from AV rind. The multi-layered cellulose nanofibers and hydrogen bonds in the chemically purified cellulose fibers were broken down by the shearing forces generated from the grinding stones. The nanometer-scale fibers were obtained in a homogenized and stable water suspension. Mechanical properties of AV rind nanofibrous films were determined and compared with those of the films prepared using wood cellulose nanofibers to evaluate the feasibility of the AV rind fibers for the production of high-strength nanofibrous films.



**Figure 1.** Image of AV leaf cross section.<sup>3</sup> [Color figure can be viewed in the online issue, which is available at [wileyonlinelibrary.com](http://wileyonlinelibrary.com).]

## MATERIALS AND METHODOLOGY

### Material

Fresh AV leaves (Southern Fields Aloe, Inc, South Texas) were used as the raw material in all experiments. Commercially available wood pulp was obtained from Tembec Inc. Reagent grade chemicals, hydrochloric acid (36%–38%, Caledon laboratories Ltd.), glacial acetic acid (Caledon laboratories Ltd.), sodium hydroxide (Caledon laboratories Ltd.), ammonium hydroxide (29.7%, J.T. Baker), sodium chlorite (nominally 80%, Alfa Aesar), 72% sulfuric acid (Ricca chemical company), and copper (II)-ethylenediamine complexes (Cuen, 1M solution in water, Acros Organics) were used as received without further purification.

### Chemical Composition Characterization of AV Rind

Extractives in AV rind were quantified using ASTM standard method D1105-96 with three steps. AV rind powder (40 mesh) was oven-dried at 105°C before extraction. The sample was extracted first with two parts of toluene to one part of 95% ethanol, followed by 95% ethanol, and boiled distilled water in the second and third extractions, respectively, to remove non-polar compounds (such as fats and resins) and polar extraneous components (such as pectin and starch). The extractive-free sample was oven dried at 105°C overnight before weighing. The percentage of extractives in AV rind can be calculated according to the following formula [eq. (1)].

$$\text{Extractives} = \frac{(W_1 - W_2)}{W_1} \times 100\% \quad (1)$$

where,  $W_1$  represents the dry weight of the AV rind before extraction; and  $W_2$  represents the dry weight of AV rind after extraction.

Chemical compositions (ash,  $\alpha$ -cellulose, hemicellulose, soluble lignin, and Klason lignin) of extractive-free AV rind powder were determined according to the procedure described by Zobel et al.<sup>7</sup> and Technical Association of the Pulp and Paper Industry (TAPPI) standard. Ash content was determined by heating a representative sample at 575°C for 4 h in a muffle furnace. Holocellulose was measured by treating in accordance with a modified acidified sodium chlorite method.<sup>8</sup> Sodium chlorite and acetic acid were added successively after the first hour and the second hour. After 3 h of heating at 70°C, the flasks were placed in an ice bath to cool the mixture below 10°C. The contents in

the flask were filtered through a tared coarse fritted glass Gooch crucible, and then washed with ice-cold distilled water, followed with hot distilled water and acetone. The treated samples were oven-dried at 105°C for 24 h before final weighing. The  $\alpha$ -cellulose was subsequently determined by a treatment with 17.5% sodium hydroxide to remove hemicellulose. Hemicellulose was calculated by the difference between holocellulose and  $\alpha$ -cellulose. Klason lignin was analyzed based on an acid hydrolysis method (adapted from TAPPI Standard T222). Soluble lignin was determined according to TAPPI UM 250 standard. Total lignin was calculated by sum of the Klason lignin and soluble lignin. The dried sample was first treated using 72% sulfuric acid solution for 1 h at 30°C, then treated in 3% sulfuric acid solution for 1 h at 121°C in an autoclave. The mixture was filtered with a pre-weighed medium crucible after cooling down. The filtrate was collected for Ultraviolet–visible (UV) spectroscopy (Evolution 60S UV–visible spectrophotometer, Thermo Fisher Scientific Inc.) analysis to determine the amount of soluble lignin at wavelength of 205 nm with an absorptivity of 110 g L<sup>-1</sup> cm<sup>-1</sup>. The insoluble residue collected was washed thoroughly with distilled water until neutral, and oven-dried at 105°C before weighing to obtain the amount of Klason lignin.

### Isolation of AV Rind Nanofibers (AVRNF)

The AV leaves were between 40 and 50 cm of length. All the leaves were washed to remove dirt from the surface. Gel inside the leaves was then removed using a knife. The rind was washed with hot water to remove the gel residue, cut into small pieces, and oven-dried at 60°C overnight. The dried pieces were milled to pass through a 2-mm screen for further treatment.

AV pulp fibers were isolated by a four-step chemical treatment as shown in Figure 2. The rind fibers were treated with 0.05N HCl solution at 70°C for 2 h to remove the extractives followed by adjusting the pH value of the mixture to 9.5 with ammonium hydroxide to remove fat and pectin. After washing, the sample obtained was air-dried, subsequently treated using 4% NaOH with solid to NaOH solution ratio of 1 : 10 (w/w) at 70°C for 2 h. Then the treated sample was bleached twice to

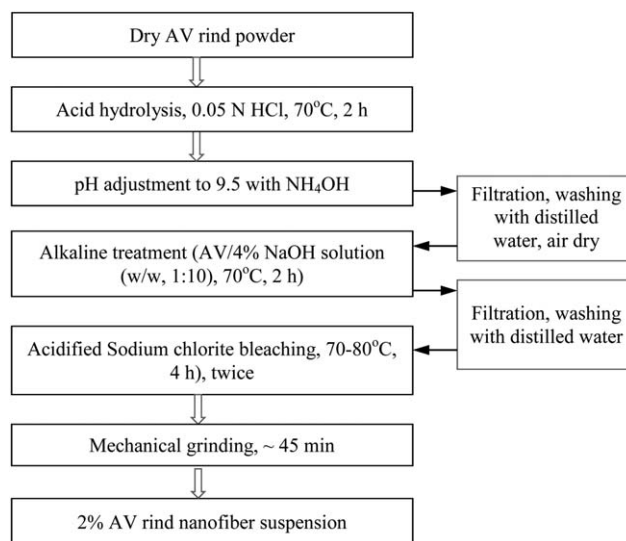


**Figure 2.** Isolation process of AVRNF.

remove lignin using an acidified sodium chlorite method as follows. In a typical run, 100 g of material, 800 mL of distilled water, 8.6 mL of glacial acetic acid, and 9 g of sodium chlorite were added to a 2 L beaker. The beaker was kept in a water bath at 70°C–80°C. After the first hour and the second hour, 9 g of sodium chlorite was added again, respectively. The beaker was then kept in this water bath for two more hours to make it 4 h in total. During the reaction, the mixture was stirred frequently. After the reaction, the beaker was cooled down to room temperature. The mixture was filtered under suction and washed thoroughly with distilled water until the washings were neutral.

After bleaching, the AV rind purified cellulose fibers were defibrillated to generate a 2% nanofiber suspension in water using a Masuko commercial grinder (Masuko Corp., Japan, 1500 rpm, about 45 min grinding) at the University of Toronto. Wood pulp was also defibrillated (about 24 min grinding) to generate a 2% nanofiber suspension as a reference as well.

#### Preparation of Nanofibrous Films

AVRNF films of thickness of 40  $\mu\text{m}$  were prepared as follows. A certain amount of AVRNF suspension was diluted with distilled water and mixed uniformly using a blender. Then the diluted suspension was filtrated using a membrane filter (0.1- $\mu\text{m}$  pores, 9 cm, Pall corporation) under suction on top with the shining surface facing up under suction to generate a film with thickness around 40  $\mu\text{m}$ . The film was dried by pressing the film in between the membranes at ambient conditions under 50 psi for 15 min. The film was finally dried at 40°C overnight before cutting mechanical test specimens that were then oven-dried at 105°C for two more hours to ensure complete drying. The obtained dried specimens were used to test the mechanical properties. Wood nanofibrous film was also prepared using similar conditions.

#### Fourier Transform Infrared Spectroscopy (FTIR) Spectra

FTIR spectrum of the sample obtained from each step in Figure 2 was examined in a KBr pellet with weight of 1 : 100 on a Bruker Tensor 27 FTIR spectrometer (Bruker Optic Inc.). The spectra were collected within the region between 4000 and 400  $\text{cm}^{-1}$ .

#### Morphological Analysis

Morphology of AV rind fibers before and after mechanical defibrillation was analyzed using Scanning electron microscopy (SEM) and Transmission electron microscopy (TEM) techniques, respectively. For preparation of SEM (JEOL Ltd., JSM-6610LV SEM, Japan) sample, a drop of diluted AV purified cellulose fibers in water solution was deposited on a carbon-coated tape on a metal stub, and dried at ambient conditions before coating with 2–3 nm of gold. AVRNF was investigated on a Hitachi H-7000 TEM (Hitachi Ltd., Japan) with an accelerated voltage of 75 kV. About 10  $\mu\text{L}$  of diluted AV solution was deposited onto glow-discharged carbon-coated TEM grids (400 mesh copper) with the excess water being removed by blotting a piece of filter paper after 2 min. Then the specimen was stained with 2% uranyl acetate solution for 2 min, and was also blotted with a piece of filter paper to remove the excess liquid. Then the specimen was dried at atmosphere for 5 min before observing.<sup>9</sup>

The diameter distribution of AVRNF obtained from TEM was calculated based on 200 individual measurements using an image processing program of ImageJ (National Institutes of Health).

#### Mechanical Properties Test of Nanofibrous Films

Tensile properties of AVRNF films were determined according to ASTM D638-10 Type V standard with the samples cut from the sheet using a standard die ASTM D-638-5-IMP-2. The mechanical properties, such as, tensile strength, Young's modulus, and percentage of elongation of the film specimens were then tested using a 3367 Universal testing machine (Instron Corp.). The tests were performed at a crosshead speed of 2.5 mm/min with a gauge length of 25 mm and load cell capacity of 2 kN. All the specimens were oven-dried at 40°C overnight before testing. At least five specimens were prepared for each sample.

#### Viscosity Average Molecular Weight ( $M_v$ ) and Average Viscometric Degree of Polymerization ( $DP_v$ )

Mark–Houwink–Sakurada (MHS) equations<sup>10</sup> of  $\eta = 0.070 M_v^{0.7} = 2.45 DP_v^{0.7}$  (where  $\eta$  is the intrinsic viscosity) were employed to investigate the  $M_v$  and  $DP_v$  of AVRNF and those of wood nanofibers. Intrinsic viscosity " $\eta$ " was examined using Huggins equation:  $\frac{\eta_{sv}}{c} = \eta + k\eta^2 c$ ; where " $\eta_{sv}$ " is the specific viscosity; " $c$ " is the concentration of different polymer solution; and " $k$ " is the Huggins constant. When the parameter of " $\eta_{sv}/c$ " is extrapolated to infinite dilution, intrinsic viscosity " $\eta$ " was obtained from " $\eta_{sv}$ " measurements through graphic extrapolations.

Four sample solutions with different concentrations ranging from 0.01 to 0.05  $\text{mL g}^{-1}$  were prepared using the 0.5M Cuen solution. The viscometric parameters were examined at room temperature (23°C  $\pm$  3°C) using a Cannon–Fenske Routine viscometer by counting the efflux time in seconds of the sample solution. " $\eta_{sv}$ " is defined as  $\eta_{sv} = \frac{t_s - t_0}{t_0}$ ; where: " $t_0$ " is the mean efflux time of the 0.5M Cuen solution; and " $t_s$ " is the mean efflux time of the sample solution.

#### X-ray Diffraction (XRD) and Crystallinity Measurement

XRD patterns of dry AV rind powder before and after chemical–mechanical treatment were determined on a Philip PW3710 X-ray Diffractometer (Philip) using a Cu-K $\alpha$  radiation ( $\lambda = 1.5406 \text{ \AA}$ ). Diffractograms were collected with a voltage of 40 kV and a current of 40 mA with a scan angle from 5° to 40° and a scan speed of 0.008 (2 $\theta$ /s). Three samples AV rind powder, AV rind purified cellulose fibers powder, and AVRNF powder were selected for XRD analyses. AV rind powder and AV cellulose fibers powder were obtained by crushing with a mortar and pestle. AVRNF powder was prepared by crushing the film prepared after treated with liquid nitrogen. All samples were dried at 40°C overnight and grinded to fine powder before measurement.

A parameter of crystallinity index (CI) is widely used to detect the relative amount of crystalline material in cellulose. CI could be defined as the ratio of the amount of crystalline cellulose to the total amount of sample material. It was calculated by means

**Table I.** Chemical Compositions of AV Rind

Chemical components	Ash (STDEV) (%)	$\alpha$ -cellulose (STDEV) (%)	Hemicellulos (STDEV) (%)	Klason lignin (STDEV) (%)	Soluble lignin (STDEV) (%)	References
AV rind	8.89 <sup>a</sup> ( $\pm 0.26$ )	57.72 <sup>b</sup> ( $\pm 2.18$ )	16.39 <sup>b</sup> ( $\pm 1.50$ )	11.40 <sup>b</sup> ( $\pm 0.28$ )	2.33 <sup>b</sup> ( $\pm 0.04$ )	This work
<i>Cereus Jamaru</i> stem <sup>c</sup>	-	21.85	20.62		3.69 <sup>d</sup>	13
<i>Opuntia ficus-indica</i> stem <sup>c</sup>	-	26.23	20.05		2.87 <sup>d</sup>	13
Empty fruit bunch of oil palm <sup>e</sup>	-	40 ( $\pm 2$ )	23 ( $\pm 2$ )		21 ( $\pm 1$ ) <sup>d</sup>	14
Kenaf core <sup>e</sup>	3.0 ( $\pm 0.4$ )	46.0 ( $\pm 0.5$ )	33.0 ( $\pm 2.0$ )		20.0 ( $\pm 1.0$ ) <sup>d</sup>	15
Eastern White pine sawdust <sup>f</sup>	0.4	40.2	21.9		28.4 <sup>d</sup>	16

<sup>a</sup>On dry and extractive-free basis.

<sup>b</sup>On dry, extractive-free, and ash-free basis.

<sup>c</sup>The cellulose was isolated by a multiple process as follows: water digestion (1 : 5, 50°C, 2 h), alkali extraction (2% NaOH, 2 h, 50°C), bleaching (2.5% NaOCl, 60°C, 2 h), and HNO<sub>3</sub> digestion (0.05N, 60°C, 1 h). The lignin analysis was achieved according to the TAPPI standard T222-03-75.

<sup>d</sup>Total lignin (Klason lignin and soluble lignin).

<sup>e</sup>The  $\alpha$ -cellulose of the Kenaf core fibers was determined by means of TAPPI test method 203 om-93. The content of hemicellulose and lignin were assessed according to the Wise and Murphy (1946) method and TAPPI standard 222 om-88, respectively.

<sup>f</sup>Cellulose and hemicellulose were determined according to TAPPI test method T249 cm-85, and the acid-soluble and acid-insoluble lignin was determined according to the TAPPI test method T222 om-88.

of the following method of “XRD peak height,” which was developed by Segal et al.<sup>11</sup>

$$CI = \frac{H_{002} - H_m}{H_{002}} \quad (2)$$

where,  $H_{002}$  is the height of the 002 peak ( $2\theta = 21.7^\circ$ ), and  $H_m$  is the height of the minimum ( $2\theta = 18.1^\circ$ ) between the 002 and the 101 peaks.

## RESULTS AND DISCUSSION

### Chemical Compositions of AV Rind

The main content in AV rind is moisture. It is as high as  $92.25\% \pm 1.50\%$  which is very consistent with a previous study<sup>12</sup> of 90% water in AV rind. The dry AV rind contained relatively high extractives content of  $25.48\% \pm 2.40\%$ . Chemical compositions of AV rind on extractive-free basis are summarized in Table I, along with other lignocellulosic resources for comparison. All the results are based on an average of three analyses.

Ash content ( $8.89\% \pm 0.26\%$ ) from this study was similar with that ( $7.12\% \pm 0.64\%$ ) from a previous study where the ash content was determined by heating overnight at 550°C using a sample of 80% ethanol insoluble residue obtained from lyophilized AV rind fraction.<sup>12</sup> But the ash content detected is much higher than that of wood (0.4% in Eastern White pine)<sup>16</sup> and Kenaf core<sup>15</sup> (3%) as shown in Table I.

The  $\alpha$ -cellulose determined in this study represented a high amount of  $57.72\% \pm 2.18\%$ . A significant amount of total lignin ( $13.73\% \pm 0.28\%$ ) was also detected in AV rind. No study has been found on determination of holocellulose ( $\alpha$ -cellulose plus hemicellulose) and total lignin (Klason lignin plus Soluble lignin) in AV rind. Only few studies investigated fibers

( $73.35\% \pm 0.3\%$ )<sup>2</sup> in dry whole AV leaves, and carbohydrates ( $60.34\% \pm 1.43\%$ ) and Klason lignin ( $19.62\% \pm 0.97\%$ )<sup>12</sup> in a sample of 80% ethanol insoluble residue obtained from lyophilized AV rind. This study shows that the AV rind had a relatively higher amount of  $\alpha$ -cellulose than Cactus materials<sup>13</sup>, wood,<sup>16</sup> and some other lignocellulosic materials<sup>14,15</sup> as shown in Table I. It suggests that AV rind has a good potential resource for isolation of natural nanofibers.

### FTIR

FTIR is used to identify types and changes of chemical bonds before and after chemical and mechanical treatment of AV rind. For close observation, the expansion of the FTIR spectra of AV rind, AV after treatment with HCl and NH<sub>4</sub>OH, AV after further treatment with NaOH, AV purified cellulose fibers, and AVRNF at wave number ranging from 1900 to 800 cm<sup>-1</sup> and resolution of 4 cm<sup>-1</sup> are represented in Figure 3.

The peaks at 1740 and 1251 cm<sup>-1</sup> ascertained the presence of the *o*-acetyl esters units, which were mostly due to hemicellulose, extractives, pectin, and lignin.<sup>17,18</sup> The peak intensity dropped after treatment with 0.05N HCl and NH<sub>4</sub>OH, which could be mostly due to the removal of extractives and fat. The peaks almost disappeared after treating with NaOH, which could be mostly attributed to the removal of hemicellulose, lignin, and pectin.<sup>19</sup> The reduction of the peaks was mainly through the de-esterification reaction during which the ester groups reacted with alkalis to form RCONH<sub>2</sub> with NH<sub>4</sub>OH and to form RCOONa with NaOH. It is worth to note that the acetyl groups were necessary for biological activation possibly due to a number of hydrophilic hydroxyl groups they covered. The hydroxyl groups will make the molecule more likely to cross the hydrophobic barriers in the cell.<sup>20</sup> Intensities at 1475, 1433, 1286, 1163, 1114, and 1039 cm<sup>-1</sup> did not significantly change



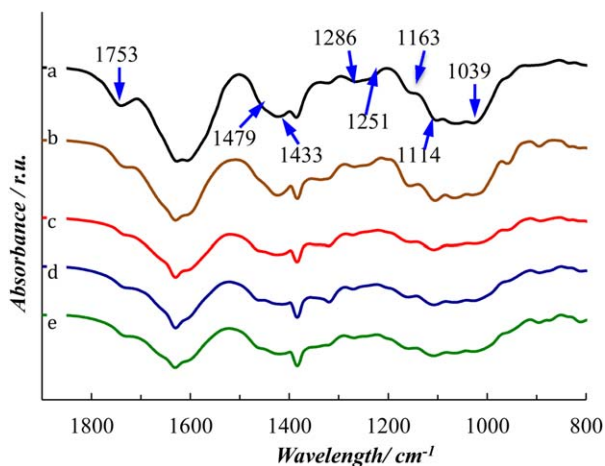


**Figure 3.** FTIR spectra of (a) AV rind; (b) After treatment with 0.05N HCl and  $\text{NH}_4\text{OH}$ ; (c) AV after further treatment with NaOH; (d) AV purified cellulose fibers; (e) AVRNF. [Color figure can be viewed in the online issue, which is available at [wileyonlinelibrary.com](http://wileyonlinelibrary.com).]

after treatment with 0.05N HCl and  $\text{NH}_4\text{OH}$ , but almost vanished after further treatment with NaOH. These bands were detected in G-type (guaiacyl kind) lignin.<sup>21</sup> The intensity drop was thus possibly due to the removal of lignin. Surprisingly,

there was no significant difference between the spectra before and after bleaching. Moreover, the lignin signal intensities were not strong in the AV rind powder. Most of the lignin has been removed through the treatment with NaOH hydrolysis. These suggest that the bleaching process needs less demanding for AVRNF isolation. However, in this study, before mechanical treatment, the bleaching processes applied aimed to remove lignin in the fibers, and to obtain a high amount of cellulose. Unfortunately, this may partly degrade and dissolve the cellulose chains to a different degree leading to a lower yield and a lower the molecular mass. The decrease in molecular mass suggests lower mechanical properties of derived products.<sup>22,23</sup>

#### Morphology of the Chemical-Purified AV Cellulose Fibers and AVRNF

Figure 4(a–d) shows the samples obtained from different steps from nanofibers isolation. It is clearly visible that the chemically purified AV cellulose fibers became white [Figure 4(c)] from brown [Figure 4(b)], suggesting the removal of lignin. A stable and homogenized nanofiber suspension in Figure 4(d) was obtained after mechanical grinding.

SEM and TEM were conducted to view the morphological changes of AV cellulose fibers before and after mechanical treatment, and the diameter size and distribution of the nanofibers.

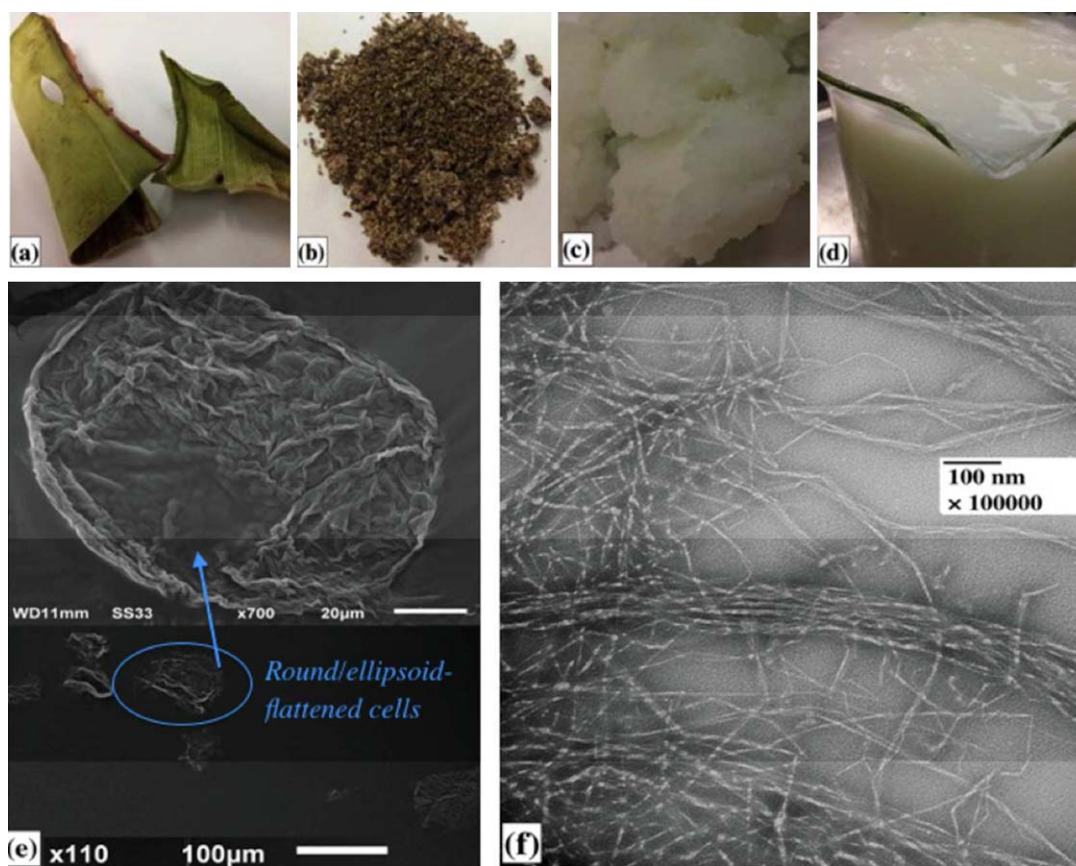


**Figure 4.** (a) Pieces of dry AV outer rind; (b) AV rind after treated with 0.05N HCl,  $\text{NH}_4\text{OH}$ , and NaOH; (c) AV purified cellulose fibers; (d) AVRNF water suspension; (e) SEM of AV purified cellulose fibers; (f) TEM of AVRNF. [Color figure can be viewed in the online issue, which is available at [wileyonlinelibrary.com](http://wileyonlinelibrary.com).]

**Table II.** Mechanical Properties of Nanofibrous Films Obtained from AV Rind, Wood, and Other Lignocellulosic Sources

Nanofibrous film	Density (g/cm <sup>3</sup> )	Tensile strength (STDEV) (MPa)	Young modulus (STDEV) (GPa)	Percentage of elongation (STDEV) (%)
AV	1.28 (±0.06)	102.12 (±10.22)	5.29 (±1.63)	7.33 (±1.44)
Wood	1.26 (±0.05)	132.90 (±8.98)	7.1 (±1.79)	11.49 (±1.57)
Rice straw <sup>a</sup>	1.36	230 (±30)	11 (±1)	-
Potato tuber <sup>a</sup>	1.34	230 (±10)	11.4 (±0.6)	-
Wood <sup>b</sup>	-	240 (±12)	11 (±0.6)	-

<sup>a</sup>Reference 26.<sup>b</sup>Reference 25.

A typical SEM image of AV purified cellulose fibers and TEM image of AVRNF are shown in Figure 4(e,f). Two hundred individual nanofibers were selected to determine the nanofibers diameter distribution.

In Figure 4(e), the SEM image clearly shows that the isolated AV rind cellulose fibers consisted essentially of round/ellipsoid-flattened cells commonly called “cell-ghosts” having different sizes with diameter generally smaller than 100 μm. Considering the AV rind anatomy structure in Figure 1, the cells were possibly the cellulose microfibrils of chlorenchyma cell wall isolated from the rind. The cellulose microfibrillar composition was clearly visualized, which was organized in a random interwoven network consisting of individual elements associated in bundles.<sup>24</sup> These authors detected similar flattened cell morphology of the “cell-ghosts” of parenchymal cells isolated from sugar beet after two-time treatment with of 2% NaOH solution at 80°C for 2 h, and a further bleaching treatment with sodium chlorite. They also reported that the TEM of the “cell-ghosts” showed the interwoven networks of the individual microfibrils with diameter size in nanometer scale.

The TEM of AVRNF was illustrated in Figure 4(f). Compared with the AV cellulose fibers, it is clearly visible that the interwoven networks of cellulose microfibrils had been completely disrupted after the mechanical treatment. Moreover, most of the elements in Figure 4(f) are nanometer-level individual fibers with few bundles. Most of the individual nanofibers diameter size was relatively uniform under 20 nm. Few larger bundles ranging from 20 to 100 nm were also detected.

### Mechanical Properties of Nanofibrous Films

Mechanical properties, such as tensile strength, Young's modulus, and percentage of elongation of the AVRNF film, the reference of wood nanofibrous film, and some other lignocellulosic materials (rice straw and potato tuber) are listed in Table II.

Compared with wood nanofibrous film, AVRNF film showed lower tensile strength, and Young's modulus for breaking. Moreover, AVRNF film had a lower percentage of elongation that means the AVRNF was more brittle than wood nanofibers. However, as shown in Table II, Panthapulakkal and Sain<sup>25</sup> who are from the same group obtained a higher tensile strength (240 ± 12 MPa) and Young's modulus (11 ± 0.6 GPa) with similar wood nanofibers. The lower mechanical properties of AV

nanofibrous film may be either due to the degradation of the fibers during the chemi-mechanical treatment or may be due to the inherent characteristics of the AV rind fibers. Degree of polymerization as well as crystallinity of these fibers were determined to investigate the lower strength of AVRNF films compared with wood cellulose nanofibers.

### Viscosity Average Molecular Weight ( $M_v$ ) and Degree of Polymerization ( $DP_v$ )

Degree of polymerization ( $DP_v$ ) and viscosity average molecular weight of the AVRNF and cellulose nanofibers were determined from the intrinsic viscosity of the respective sample solutions. Figure 5 represents the relation between “ $\eta_{sp}/c$ ” and “ $c$ ” obtained for AVRNF and the reference of wood nanofibers.

A linear relation was observed for both samples. Intrinsic viscosity “ $\eta$ ” was attained by graphic extrapolation. Wood nanofibers had a larger “ $\eta$ ” than AVRNF. The “ $M_v$ ” and “ $DP_v$ ” value of wood nanofibers were much larger than those of AVRNF as shown in Table III. The decrease in molecular mass suggests lower mechanical properties of derived products.<sup>27,28</sup> Iwamoto et al.<sup>29</sup> pointed out that the degree of polymerization and degree of crystallinity of cellulose fibers decreased with increasing the number of passes through the mechanical grinder. It indicates that degree of polymerization and degree of crystallinity of cellulose depends on the high shear applied

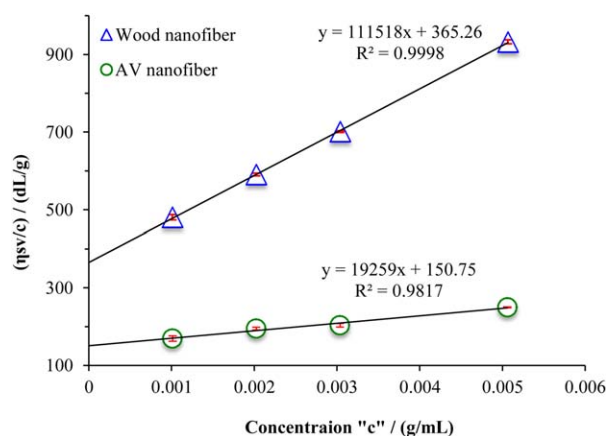


**Figure 5.** Huggins plots for AV nanofibers and wood nanofiber solutions in 0.5M Cuen solution at 23°C ± 3°C. [Color figure can be viewed in the online issue, which is available at [wileyonlinelibrary.com](http://wileyonlinelibrary.com).]

**Table III.** Intrinsic Viscosity “ $\eta$ ”, Viscosity-Average Molecular Weight “ $M_v$ ” and Average Viscometric Degree of Polymerization “ $DP_v$ ” of AVRNF and Wood Nanofibers in 0.5M Cuen Solution at  $23^\circ\text{C} \pm 3^\circ\text{C}$

Origin	$\eta$ (mL/g)	$M_v$ (g/mol)	$DP_v$
AV nanofibers	161.18 ( $\pm 3.43$ )	61,594 ( $\pm 1929$ )	396 ( $\pm 12$ )
Wood nanofibers	370.03 ( $\pm 4.77$ )	208,345 ( $\pm 3833$ )	1297 ( $\pm 24$ )

on the cellulosic resource during grinding. Thus, the low value of  $DP_v$  of AVRNF could be caused by the damage of the AV rind fibers during grinding (longtime grinding in the grinder compared with wood fibers). Furthermore, as mentioned above, the pulping and bleaching process could also degrade and dissolve the cellulose chain, which would result in the low value of  $M_v$  and  $DP_v$  of AVRNF. These results demonstrated that the lower mechanical properties of the AVRNF film compared with the wood nanocellulose fiber films might be due to the AV rind cellulose with a lower degree of polymerization. Further research is needed to explicitly differentiate if the lower degree of polymerization is caused by the chemical treatment or mechanical grinding and would be included in the future studies.

#### XRD and Crystallinity

Three samples, AV rind powder, AV cellulose fibers powder, and AVRNF powder, were selected for XRD analysis to investigate the effect of chemical–mechanical treatment on their crystalline structure. The XRD patterns of the three samples are shown in Figure 6.

As shown in Figure 6, AV rind powder had relatively broader peaks than AVRNF and AV cellulose fibers powder. The two overlapped peaks at  $2\theta = 14.6^\circ$  and  $15.7^\circ$  were not observed even in AV rind powder. An important assumption to XRD analysis is that peak broadening is mainly contributed by the increased amorphous contributor. AV rind mainly contains cellulose and amorphous matrix structure of hemicellulose, pectin, and lignin. Cellulose consists of ordered crystalline and disordered amorphous regions. Moreover, plant-derived cellulose is generally detected in a mixture with hemicellulose, lignin, pectin, and other substances.<sup>29</sup> All these might cause the broader peak of AV rind powder. AV cellulose fibers and AVRNF displayed very similar diffraction spectra. Both samples showed a primary peak at  $2\theta = 21.7^\circ$  and two overlapped peaks at  $2\theta = 14.6^\circ$  and  $15.7^\circ$  from diffraction on the cellulose I's 110,  $1\bar{1}0$ , and 002 planes, respectively.<sup>30–32</sup> There was only the main peak at  $2\theta = 21.2^\circ$  from cellulose I for AV rind powder.

It is also worth to mention that all three samples showed small sharp peaks at  $2\theta = 14.9^\circ$ ,  $24.2^\circ$ ,  $29.9^\circ$ , and  $38.1^\circ$  which were assigned to be the  $\bar{1}01$ , 020,  $\bar{2}02$ , and 130 of calcium oxalate monohydrate, respectively.<sup>33,34</sup> Some researchers from University of Miami School of Medicine and University of Mississippi also found calcium oxalate crystal in AV.<sup>3,35</sup> Femenia et al.<sup>12</sup> reported that calcium was the main mineral element in AV.

CI, calculated using eq. (2), of AVRNF along with wood nanofibers are represented in Table IV. Wood nanofibers<sup>25</sup> had a higher CI (0.90) than AVRNF (CI of 0.66). The cellulose fibrils with a high degree of polymerization were expected to have a high crystallinity. The lower crystallinity of the AVRNF can be attributed to the lower degree of polymerization compared with the wood nanocellulose films. A higher crystallinity suggests higher mechanical properties of the fibers and the derived products. It is consistent with the mechanical properties results of the nanofibrous films in Table II. Wood nanofibrous film performed better mechanical properties than AVRNF film. Rice straw and potato straw nanofibers<sup>26</sup> represented higher CI (shown in Table IV) than AVRNF. And the films generated with their nanofibers also had higher tensile properties (shown in Table II) than AVRNF.

It is also worth to mention that CIs of the AV pulp and AVRNF were calculated to be 0.59 and 0.66, respectively. The result indicate that the mechanical defibrillation introduced a crystallinity increase to the AVRNF compared with the AV purified cellulose fibers. Similar results were obtained in some previous research.<sup>25,26,36,37</sup> The reason could be that the amorphous cellulose was degraded during the mechanical defibrillation, and removed by filtration during the film preparation.

Several possible reasons regarding the low mechanical properties of AVRNF film could be explained here. (1) One reason could be the different pulping and bleaching processes employed. AV fibers in this study were bleached twice with an acidified sodium chlorite at  $70^\circ\text{C}$ – $80^\circ\text{C}$  for 4 h due to the light yellow color of the pulp after the first bleaching. It was assumed to be the lignin residue. The two-bleaching treatment might increase the attack on carbohydrates degradation and dissolution during delignification. The acid employed could contribute to carbohydrate degradation. Wood pulp obtained from Tembec was derived from a Totally Chlorine Free (TCF) bleaching process. Abe and Yano<sup>26</sup> used another different pulping and bleaching process. Moreover, compared with wood and other agricultural materials, AV rind had a lower lignin content as shown above in Table I. The FTIR spectra analyses

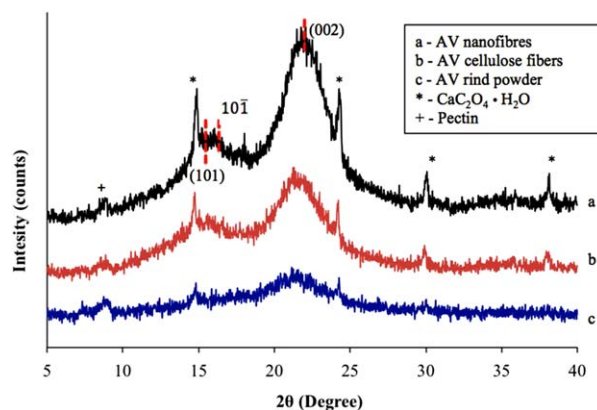


**Figure 6.** XRD patterns of AV rind powder, AV cellulose fibers, and AVRNF. [Color figure can be viewed in the online issue, which is available at [wileyonlinelibrary.com](http://wileyonlinelibrary.com).]



**Table IV.** CI of AV Pulp, AVRNF, Wood Nanofibers, and Other Nanofibers from Different Sources

Sources	AV pulp	AVRNF	Wood nanofiber <sup>a</sup>	Rice straw <sup>b</sup>	Potato straw <sup>b</sup>
CI	0.59	0.66	0.90	0.76	0.80

<sup>a</sup>Reference 25.<sup>b</sup>Reference 26.

also showed that there was no significant difference regarding the lignin amount before and after bleaching. These indicate that the bleaching treatment for AV rind would need less demanding; (2) Cellulose microfibrils in agricultural fibers are less tightly wound in the primary cell than in the secondary wall in wood.<sup>38</sup> It means the mechanical defibrillation to produce nanofibers from AV rinds should need less energy demanding. Furthermore, the long-time grinding (about 45 min) could also cause the low degree of crystallinity and degree of polymerization.<sup>29</sup> Therefore, the long grinding time for defibrillation of AVRNF may correspond to the lower mechanical properties of the film; (3) Panthapulakkal and Sain<sup>25</sup> obtained a higher tensile strength (240 ± 12 MPa) and Young's modulus (11 ± 0.6 GPa) with the same wood nanofibers, that illustrates that the film preparation process hired in this work may also need to be improved; (4) The higher density of nanofibrous films prepared by Abe and Yano<sup>26</sup> could be another reason for the higher tensile strength. All these could cause the lower mechanical properties of the AVRNF film. Therefore, the optimum nanofibers isolation process and film preparation process need to be investigated in further study.

## CONCLUSIONS

This study was a preliminary attempt to develop nanofibers and nanofibrous films from AV rind part. The results demonstrated a high amount of  $\alpha$ -cellulose in AV rind, suggesting that AV rind could be used fully for isolation of nanofibers rather than discarded. Most of isolated fibers were individual nanometer scale fibers with diameter under 20 nm. The bleaching should hire less harsh treatment for isolation of AVRNF through the FTIR analyses. Lower mechanical properties of AVRNF films compared with wood cellulose nanofibrous films was attributed to the low crystallinity, molecular weight, and degree of polymerization of the AVRNF. The above-mentioned lower characteristics may be caused by the damage occurred to the AV rind fibers during chemical as well as mechanical treatments. More studies are required to differentiate the structural changes occurred to the AV rind fibers during the nanofiber isolation. Further in order to improve the mechanical properties, the optimum nanofibers isolation processes, such as pulping, bleaching, mechanical defibrillation, and film preparation, has to be performed. These would be the subjects of further studies.

## ACKNOWLEDGMENTS

The authors are grateful for the financial support from the Natural Sciences and Engineering Research Council of Canada (NSERC) and King Abdulaziz University.

## REFERENCES

- Moghaddasi, S. M.; Verma, S. K. *Int. J. Biol. Med. Res.* **2011**, *2*, 466.
- Ahmed, M.; Hussain, F. *Int. J. Chem. Biochem. Sci.* **2013**, *3*, 29.
- Klein, A. D.; Penneys, N. S. *J. Am. Acad. Dermatol.* **1988**, *18*, 714.
- Eshun, K.; He, Q. *Cri. Rev. Food Sci. Nutr.* **2004**, *44*, 91.
- Choi, S. W.; Son, B. W.; Son, Y. S.; Park, Y. I.; Lee, S. K.; Chung, M. H. *Br. J. Dermatol.* **2001**, *145*, 535.
- Davis R. H. *Comments on the aloe leaf*. **1992**. <http://www.desertharvest.com/physicians/documents/203-0.pdf>.
- Zobel, B. J.; Stonecypher, R.; Brown, C.; Kellison, R. C. *TAPPI* **1966**, *49*, 383.
- Sun, J. X.; Sun, X. F.; Zhao, H.; Sun, R. C. *Polym. Degrad. Stab.* **2004**, *84*, 331.
- Jiang, F.; Han, S. Y.; Hsieh, Y. L. *RSC Adv.* **2013**, *3*, 12366.
- Kes, M.; Christensen, B. E. *J. Chromatogr. A* **2013**, *1281*, 32.
- Segal, L.; Creely, J. J.; Martin, A. E.; Conrad, C. M. *Text. Res. J.* **1959**, *29*, 786.
- Femenia, A.; Sanchez, E. S.; Simal, S.; Rossello, C. *Carbohydr. Polym.* **1999**, *39*, 109.
- Monye, M. S. Master dissertation. North-West University, Potchefstroom Campus. **2012**. <http://hdl.handle.net/10394/8057>.
- Jonoobi, M.; Khazaeian, A.; Tahir, P. M. SaifulAzry, S.; Oksman, K. *Cellulose* **2011**, *18*, 1085.
- Jonoobi, M.; Harun, J.; Tahir, P. M.; Zaini, L. H.; SaifulAzry, S.; Makinejad, M. D. *BioResources* **2010**, *5*, 2556.
- Cheng, S.; D'cruz, I.; Wang, M. C.; Leitch, M.; Xu, C. *Energy Fuels* **2010**, *24*, 4659.
- Himmelsbach, D.; Khalili, S.; Akin, D. *J. Sci. Food Agric.* **2002**, *82*, 685.
- Íñiguez1, G.; Valadez, A.; Manríquez, R.; Moreno, M. V. *Rev. Int. Contam. Ambie.* **2011**, *27*, 61.
- Sain, M., Panthapulakkal, S. *Ind. Crops Prod.* **2006**, *23*, 1.
- Reynolds, T.; Dweck, A. C. *J. Ethnopharmacol.* **1999**, *68*, 3.
- Derkacheva, O.; Sukhov, D. *Macromol. Symp.* **2008**, *265*, 61.
- Sookne, A. M.; Harris, M. *Ind. Eng. Chem.* **1945**, *37*, 478.
- Berggren, R. Doctoral Thesis, *Royal Institute of Technology*. **2003**.
- Dinand, E.; Chanzy, H.; Vignon, M. R. *Cellulose* **1996**, *3*, 183.
- Panthapulakkal, S.; Sain, M. *Int. J. Polym. Sci.* **2011**, *2012*, 4.
- Abe, K.; Yano, H. *Cellulose* **2009**, *16*, 1017.
- Sookne, A. M.; Harris, M. *Ind. Eng. Chem.* **1945**, *37*, 478.
- Berggren, R. Doctoral Thesis, *Royal Institute of Technology*. **2003**.
- Iwamoto, S.; Nakagaito, A. N.; Yano, H. *Appl. Phys. A* **2007**, *89*, 461.
- Zhang, J.; Kamdem, D. P. *Holzforchung* **2000**, *54*, 27.



31. Borysiak, S.; Doczekalska, B. *Fibres Text. East. Eur.* **2005**, *13*, 87.
32. Nishio, Y.; Manley, R. S. *J. Macromolecules* **1988**, *21*, 1270.
33. Ouyang, J. M.; Deng, S. P.; Zhong, J. P.; Tieke, B.; Yu, S. H. *J. Cryst. Growth* **2004**, *270*, 646.
34. Deng, S. P.; Zheng, H.; Ouyang, J. M. *Mater. Sci. Eng. C* **2006**, *26*, 683.
35. Odeleye, O. M.; Elujoba, A. A.; Gbolade, A. A. 8th Annual Oxford International Conference on the Science of Botanicals. University of Mississippi. April 6, **2009**.
36. Cheng, Q. Z.; Wang, S. Q.; Rials, T. G.; Lee, S. H. *Cellulose* **2007**, *14*, 593.
37. Cheng, Q. Z.; Wang, S. Q.; Han, Q. Y. *J. Appl. Polym. Sci.* **2010**, *115*, 2756.
38. Siro, I.; Plackett, D. *Cellulose* **2010**, *17*, 459.